The Resonance Raman Spectrum of Hexakis(dimethylamido)Tungsten(VI)

ROBIN J. H. CLARK and TREVOR J. DINES

Christopher Ingold Laboratories, University College London, 20 Gordon Street, London WC1H 0AJ, U.K.

Received July 21, 1982

The Raman and resonance Raman spectra of $W(NMe_2)_6$ in cyclohexane solution at room temperature and as a KBr disc at ca. *80 K have been recorded using laser excitation in the range 337.5–568.2 nm. The resonance Raman spectrum displays bands assigned to vibrational fundamentals of the $W(NC_2)_6$ framework, a band assigned to CH_3 deformation, and overtones and combination bands of these. An approximate force constant calculation is presented for the modes associated with the $W(NC_2)_6$ framework. The excitation profiles for the bands assigned to the fundamental modes all maximize close to the absorption maximum associated with the lowest allowed electronic transition at 363 nm as expected for the A-term scattering regime in the small displacement approximation.*

Introduction

The chemistry of transition metal dialkylamides has received considerable attention in the past decade [1–3]. Such compounds, of type ML_n (where L = NR_2), are known for all of the Groups IV, V and VI transition metals for certain values of n. However, the only compound to be synthesized for which n = 6 is hexakis(dimethylamido)tungsten(VI), $W(NMe_2)_6$. The molecular structure of $W(NMe_2)_6$ has been shown by an X-ray crystallographic study to have T_h geometry [4]. $W(NMe_2)_6$ is red, due to an intense electronic absorption band in the near-u.v. region, which tails into the visible region of the spectrum. This band is assigned to the lowest allowed nitrogen-to-tungsten charge-transfer transition, $^1T_u \leftarrow {}^1A_g$ ($t_u^5 t_g^1 \leftarrow t_u^6$). Infrared and Raman spectra of $W(NMe_2)_6$ and its perdeuterated analogue each display five bands in the 300–1000 cm^{-1} region [3] (the infrared and Raman bands wavenumbers do not coincide, as expected for a centrosymmetric molecule). All of the observed infrared and Raman bands shift markedly to lower wavenumber on deuteration, thus implying extensive contributions from several symmetry coordinates in each normal coordinate.

The purpose of the present study is two-fold: (a) to obtain improved infrared and Raman spectroscopic data, thereby enabling a vibrational analysis to be performed, and (b) to obtain Raman measurements for excitation resonant with the ligand-to-metal charge-transfer transition of lowest energy, in order that the molecular geometry changes attendant upon this transition be revealed.

Experimental

Raman spectra of $W(NMe_2)_6$ were obtained from a cyclohexane solution (*ca.* 10^{-2} *M*) in a spinning cell, and from a KBr disc held at *ca.* 80 K. The latter required the use of a cylindrical lens to produce a line focus of the exciting laser beam in order to prevent decomposition of the sample.

A Spex 14018 (Ramalog 6) spectrometer interfaced to a Nicolet 1180 computer was used to record the Raman spectra, which were excited by laser lines in the range 337.5–568.2 nm from Coherent Radiation Model CR15UV argon ion and CR3000K krypton ion lasers. Band wavenumber measurements were calibrated using the emission spectrum of neon, and band intensities, determined as the product of peak height and full-width-at-half-maximum (F.W.H.M.), were corrected for the spectral response of the spectrometer. Depolarization measurements involving u.v. excitation were obtained using a Polaroid HNP'B linear polarizer.

Infrared spectra were recorded from nujol and hexachlorobutadiene mulls using a Perkin-Elmer 225 spectrophotometer and electronic absorption spectra were obtained from a cyclohexane solution in a silica cuvette using a Cary 14 spectrophotometer.

Results

The Raman spectrum of a solution of $W(NMe_2)_6$ in C_6H_{12} was recorded using excitation in the range 337.5–568.2 nm. For excitation within the contour

0020-1693/83/0000-0000/$03.00

TABLE I. Details of the Raman Spectrum of $W(NMe_2)_6$.

Assignment	Wavenumber/cm^{-1}		
	C_6H_{12} soln. (λ_0 = 350.7 nm)	($\rho_\perp(\pi/2)$)	CsI disc, 80 K (λ_0 = 476.2 nm)
ν_6 (e_g), $\delta(C_2N)$	331.8 ± 1	(0.75)	338.5 ± 0.5
ν_3 (a_g), $\delta(C_2N)$	351.7 ± 1	(0)	361.7 ± 0.5
ν_2 (a_g), $\nu_s(WN)$ / ν_5 (e_g), $\nu_{as}(WN)$	553.9 ± 0.5	(0.33)	550.1 ± 0.5
ν_4 (e_g), $\nu_{as}(C_2N)$	957.5 ± 0.5	(0.75)	963.3 ± 0.5
ν_1 (a_g), $\nu_s(C_2N)$	982.2 ± 1	(0)	991.2 ± 0.5
$\delta(CH_3)$	1221.1 ± 0.5	(0.33)	1222.4 ± 0.5
	1410.6 ± 1		
$\nu_2 + \nu_4$ (E_g)	1510.6 ± 1		
$\nu_1 + \nu_2$ (A_g)	1546.2 ± 1		
$\nu_2 + \delta(CH_3)$	1773 ± 1		1773.2 ± 1
$2\nu_4$ ($A_g + E_g$)	1914 ± 1		
$\nu_4 + \delta(CH_3)$	2179.5 ± 1		
$\nu_1 + \delta(CH_3)$	2204 ± 2		

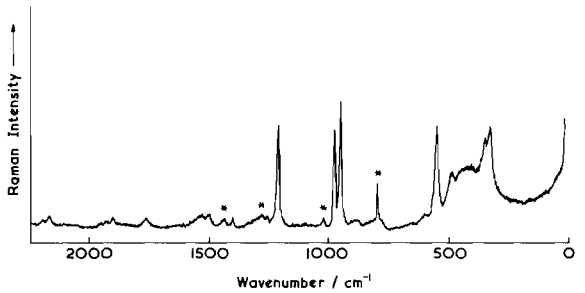

Fig. 1. Resonance Raman spectrum of $W(NMe_2)_6$ in cyclohexane solution recorded with 350.7 nm excitation. Power at the sample = 100 mW, scan speed = 1 cm^{-1} s^{-1}, time constant = 1 s, integration time = 0.5 s and spectral slitwidth = 5 cm^{-1} at 350.7 nm. The bands marked * are due to the solvent and the broad features centred on *ca.* 450 cm^{-1} and *ca.* 800 cm^{-1} are due to Raman scattering from the silica cell.

of the lowest energy electronic absorption band at λ_{max} = 363 nm (ϵ_{max} = 4010 m^2 mol^{-1} = 40,100 M^{-1} cm^{-1}) resonance Raman spectra are observed, the band intensities being about two orders of magnitude greater than for excitation well removed from the absorption band (*e.g.* 568.2 nm). The resonance Raman spectrum obtained with 350.7 nm excitation is shown in Fig. 1 and the band wavenumber measurements and assignments are presented in Table I. Additionally, Raman spectra of $W(NMe_2)_6$ were obtained from a sample dispersed in a KBr disc held at a nominal 80 K. Although this sample decomposed when excited under resonance conditions, good

TABLE II. Details of the Infrared Spectrum of $W(NMe_2)_6$.

Assignment	Wavenumber/cm^{-1}
ν_{18} (t_u), $\delta(C_2N)$	322 vw
ν_{17} (t_u), $\delta(WN_6)$	362 w
ν_{16} (t_u), $\delta(WN_6)$	420 w
ν_{15} (t_u), $\nu(WN)$	545 s
ν_{14} (t_u), $\nu(C_2N)$	944 vs

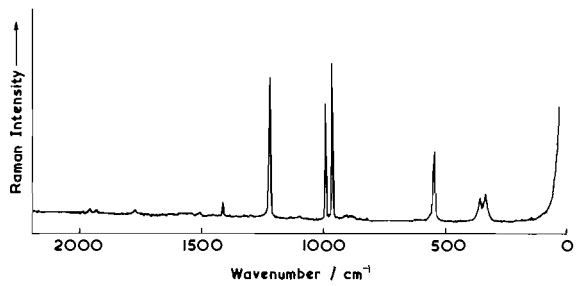

Fig. 2. Raman spectrum of $W(NMe_2)_6$ in a CsI disc at 80 K recorded with 476.2 nm excitation. Power at the sample = 100 mW, scan speed = 1 cm^{-1} s^{-1}, time constant = 1 s, integration time = 0.5 s and spectral slitwidth = 2.5 cm^{-1} at 476.2 nm.

quality spectra were obtained for excitation off-resonance; a representative spectrum, recorded using 476.2 nm excitation, is shown in Fig. 2 and

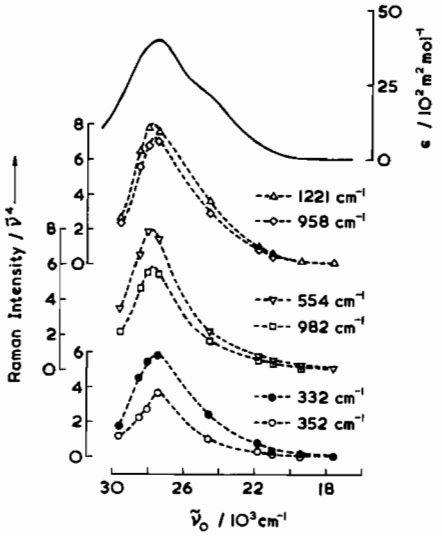

Fig. 3. Excitation profiles and electronic absorption spectrum of $W(NMe_2)_6$ in cyclohexane solution.

the band wavenumber measurements are listed in Table I.

Resonance Raman excitation profiles were constructed for the six most intense bands of $W(NMe_2)_6$, using the 802 cm^{-1} band of C_6H_{12} as an internal intensity standard. These are shown in Fig. 3, together with the electronic absorption spectrum of the solution.

Infrared measurements were obtained from samples dispersed in nujol and hexachlorobutadiene mulls. The bands wavenumber measurements and assignments are given in Table II; these are essentially identical to the results of Bradley *et al.* [3].

Discussion

Vibrational Analysis

The molecular point group of $W(NMe_2)_6$ is T_h and the symmetry species of the molecular vibrations are as follows:

WN_6 framework: $\Gamma = a_g + e_g + t_g + 3t_u$

$(NC_2)_6$: $\Gamma = 2a_g + 2e_g + 4t_g + a_u + e_u + 5t_u$

$(CH_3)_{12}$: $\Gamma = 5a_g + 5e_g + 13t_g + 4a_u + 4e_u + 14t_u$

Since the molecule is centrosymmetric the mutual exclusion rule applies; the Raman-active modes are of a_g, e_g and t_g symmetry, the t_u modes are infrared active and the a_u and e_u modes are inactive. However, the numbers of infrared and Raman bands observed, as summarized in Tables I and II, are far fewer than expected. The basis for the proposed assignments is as follows:

(1) The bands assigned to the metal–nitrogen stretching modes in the infrared spectra of a number of tetrahedral metal dimethylamides $M(NMe_2)_4$ (M = Ti, Zr, Hf, V, Nb, Ta) lie in the region 528–595 cm^{-1} [5] and those for a wide range of metal–ammines occur in a similar region [6]. It is therefore reasonable to assign the Raman band at 554 cm^{-1} to ν_s(W–N) and the i.r. band at 545 cm^{-1} to ν_{as} (W–N). (*cf.* for WCl_6, ν_s (a_{1g}) is at 410 cm^{-1} and thus at higher wavenumber than ν_{as} (t_{1u}) which is at 364 cm^{-1} [7].

(2) The assignment of the $\nu(C_2N)$ and $\delta(CH_3)$ modes is justified on the grounds that these occur in the regions 943–950 cm^{-1} and 1236–1250 cm^{-1}, respectively, in the $M(NMe_2)_4$ compounds [5].

(3) The two bands at 332 and 352 cm^{-1} in the Raman spectrum could be assigned either to $\delta(NC_2)$ or to $\delta(WN_6)$ modes. We prefer the former on the grounds that only a single depolarized $\delta(WN_6)$ mode is Raman active whereas there are two Raman-active $\delta(NC_2)$ modes to be expected, one polarized and the other depolarized. This is what we observe experimentally. Moreover, the $\delta(NC_2)$ bands are expected to be resonance enhanced since, on excitation, the equilibrium NC_2 bond angle would be expected to increase significantly (*vide infra*). A single infrared-active $\delta(NC_2)$ fundamental is expected, which we believe gives rise to the 322 cm^{-1} band.

(4) The two remaining infrared bands, at 362 and 420 cm^{-1}, are believed to arise from the two asymmetric deformation modes of the WN_6 moiety. One of these is analogous to the t_{1u} (infrared active) mode of an octahedral MX_6 system and the other corresponds to the inactive t_{2u} mode. For almost all octahedral molecules the t_{2u} mode is of lower wavenumber than the t_{1u} mode and it is for this reason that we assign the 362 cm^{-1} band as the t_{2u} analogue and the 420 cm^{-1} band as the t_{1u} analogue.

In an earlier study of the infrared and Raman spectra of $W(NMe_2)_6$, Bradley *et al.* [3] showed that all bands shift markedly to lower wavenumber ($\geqslant$10%) on deuteration, a situation which was also found to be the case for $W_2(NMe_2)_6$ [8]. This demonstrates that the vibrational modes associated with the $W(NC_2)_6$ framework are extensively coupled to other vibrational modes associated with the CH_3 groups. A straightforward vibrational assignment is therefore not possible and the mode descriptions proposed in Tables I and II can only be regarded as approximate. Nevertheless, we have attempted to perform a limited, albeit very approximate, force constant analysis by assuming that the vibrational modes of the $W(NC_2)_6$ framework may be treated separately from those of the methyl groups. Notwithstanding this assumption a general valence force field (GVFF) requires 86 force constants to be fitted to 5 Raman and 5 infrared band wavenumbers. This is obviously

TABLE III. Approximate Force Constants for $W(NMe_2)_6$.

(i) ν(W–N)	
f_r/mdyn Å^{-1}	2.48
$f_{rr'}$/mdyn Å^{-1}	0.35
$f_{rr'}$ refers to a *trans* pair of W–N bonds.	
(ii) ν(C–N)	
f_s/mdyn Å^{-1}	3.79
f_{ss}*/mdyn Å^{-1}	0.72
f_{ss}/mdyn Å^{-1}	0.02
f_{ss}* refers to a pair of C–N bonds possessing a common N atom and f_{ss} refers to a pair of C–N bonds attached to *cis* W–N bonds.	
(iii) $\delta(NC_2)$	
f_α/mdyn Å^{-1}	0.46
$f_{\alpha\alpha}$/mdyn Å^{-1}	0.01
$f_{\alpha\alpha'}$/mdyn Å^{-1}	0.05
$f_{\alpha\alpha}$ and $f_{\alpha\alpha'}$ refer, respectively, to C$\hat{N}$C bond angles involving *cis* and *trans* W–N bonds.	

an impossible calculation and it has been necessary to equate all but a small number of the force constants to zero, especially those involving NC_2 wagging, rocking and twisting modes (since no bands attributable to these were observed) as well as most of the interaction force constants. The symmetry coordinates and F and G matrix elements associated with the $W(NC_2)_6$ framework are presented in the Appendix, and the results of the force constant calculations are summarized in Table III.

The Raman data obtained from the cyclohexane solution were used in preference to those obtained from the solid because the former are expected to be closer to the values for the isolated molecule. However, the Raman spectrum of the solid does not differ greatly from the solution spectrum, and no site group or factor group splittings are observed. This is to be expected as the space group is Im3 (T_h^5), with one molecule per primitive unit cell, and therefore the factor group and site group are the same as the molecular point group.

The assignments of the bands observed in the 1400–2200 cm^{-1} region of the resonance Raman spectrum to overtone and combination tones are proposed for two reasons: first, because these bands are all much less intense than those observed in the 300–1250 cm^{-1} region (which obviously arise from fundamentals), and second, because these bands are in all cases only a few cm^{-1} below the arithmetical sums of the wavenumbers of the appropriate fundamentals. This would suggest that the relevant anharmonicity constants x_{ii} and x_{ij} are all negative, which is usually found to be the case.

Depolarization Ratios

For molecules of T_h symmetry the depolarization ratios for excitation at resonance should be as follows: a_g $\rho_\perp(\pi/2) = 0$, e_g $\rho_\perp(\pi/2) = 0.75$ and t_g $0.75 \leqslant \rho_\perp(\pi/2) \leqslant \infty$. Anomalous polarization for t_g modes arises because both symmetric and antisymmetric tensor components transform as this representation. Thus the absence of any anomalously polarized bands in the resonance Raman spectrum of $W(NMe_2)_6$ supports our assignment of all non-totally symmetric modes as being of e_g type. The polarized bands in the resonance Raman spectrum have depolarization ratios of either zero or 0.33. However, since the ground state of $W(NMe_2)_6$ possesses neither orbital nor spin degeneracy, a totally symmetric Raman band must necessarily have a depolarization ratio of zero. That this is not so for the 553.9 and 1221.1 cm^{-1} bands leads us to suggest that in these cases, a_g bands are overlapped by e_g bands. A similar situation occurs with Se_4^{2+} and Te_4^{2+} [9], for which the band wavenumbers of the a_{1g} ($\rho_\perp(\pi/2) = 0.125$) and b_{2g} ($\rho_\perp(\pi/2 = 0.75$) stretching modes coincide, leading to an overall band depolarization ratio of 0.33 in each case [9]. The assignment of the 553.9 cm^{-1} band to an overlap of the a_g and e_g metal–nitrogen stretching modes would require that the force constant f_{rr} (relating to *cis* W–N bonds) be zero, and the intensity ratio $I(\nu_2)/I(\nu_5)$ be 0.71.

Electronic Absorption Spectrum and Excitation Profiles

The electronic absorption band at 363 nm is assigned to a ligand-to-metal charge-transfer transition resulting from the transfer of an electron from a t_u orbital localized on the ligands to a t_g orbital which is metal–ligand anti-bonding. Such an electron transfer gives rise to two electric-dipole-allowed transitions of the type $^1T_u \leftarrow {}^1A_g$. It is likely that the shoulder observed at *ca.* 410 nm represents one of these transitions and the peak at 363 nm the other.

The resonance Raman excitation profiles of the six observed fundamentals ($\delta(C_2N)$ at 331 and 352 cm^{-1}, $\nu(C_2N)$ at 958 and 982 cm^{-1}, ν(WN) at 554 cm^{-1} and $\delta(CH_3)$ at 1221 cm^{-1}) are practically identical in shape and all maximise close to the absorption band maximum. No features associated with the 410 nm shoulder in the absorption spectrum are observed. That the intensities of the e_g modes are comparable with those of the a_g modes, coupled with the fact that overtones and combination bands are very weak, indicates that the molecule undergoes little change in geometry in the resonant excited state. The e_g modes may acquire intensity, either

due to Jahn–Teller coupling within the degenerate excited state, or by Herzberg–Teller coupling of the resonant state to a second state, possibly that involved in the electronic transition giving rise to the shoulder at 410 nm. The scattering mechanism for the a_g modes may be either Herzberg–Teller (B-term) or Franck–Condon (A-term) but the appearance of overtones and combination bands would tend to suggest the latter. Likewise, the appearance of combination bands and an overtone band involving e_g modes favours the Jahn–Teller mechanism for the intensification of e_g modes at resonance. That the overtones are weak indicates that the geometric changes attendant upon excitation are small along any one coordinate and distributed over the whole of the $W(NC_2)_6$ framework, as is normally the case for large polyatomic molecules [10, 11]. The nature of the resonance-enhanced bands indicates that those structural changes which do occur on excitation are, not surprisingly, concentrated along the CN and WN bonds and the C_2N and H_3C angles. The sense of the structural changes on excitation (in view of the nature of the resonant transition) is to increase the WN bond lengths. Moreover, as the CNC angles (103°) in this compound are smaller than for other dimethylamido compounds (*e.g.* 111° for $W_2(NMe_2)_6$ and 112° for $Ti(NMe_2)_2(O_2CNMe_2)_2$) [8, 12], presumably as a consequence of significant steric congestion in the molecule, one can speculate that these angles would increase in the excited state (for which the steric congestion is reduced).

Acknowledgements

The authors thank the Science Research Council and the University of London for financial support, and Professor D. C. Bradley for supplying the pure sample.

References

1 D. C. Bradley and M. H. Chisholm, *Acc. Chem. Res.*, *9*, 273 (1976).
2 D. C. Bradley, M. H. Chisholm, M. W. Extine and M. E. Stager, *Inorg. Chem.*, *16*, 1794 (1977).
3 D. C. Bradley, M. H. Chisholm and M. W. Extine, *Inorg. Chem.*, *16*, 1791 (1977).
4 D. C. Bradley, M. H. Chisholm, C. E. Heath and M. B. Hursthouse, *J Chem. Soc. Chem. Comm.*, 1261 (1969).
5 D. C. Bradley and M. H. Gitlitz, *J. Chem. Soc. A*, 980 (1969).
6 R. J. H. Clark and C. S. Williams, *J. Chem. Soc. A*, 1425 (1966).
7 W. van Bronswyk, R. J. H. Clark and L. Maresca, *Inorg. Chem.*, *8*, 1395 (1969).
8 M. H. Chisholm, F. A. Cotton, M. W. Extine and B. R. Stults, *J. Am. Chem. Soc.*, *98*, 4477 (1976).
9 R. J. H. Clark, T. J. Dines and L. T. H. Ferris, *J. Chem. Soc. Dalton*, 2237 (1982).
10 J. R. Campbell, R. J. H. Clark, W. P. Griffith and J. P. Hall, *J. Chem. Soc. Dalton*, 2228 (1980).
11 R. J. H. Clark and T. J. Dines, *Mol. Phys.*, *42*, 193 (1981).
12 M. H. Chisholm and M. W. Extine, *J. Am. Chem. Soc.*, *99*, 792 (1977).

Appendix

Symmetry coordinates and F and G matrix elements used in the force constant calculations.

The symmetry coordinates for the $W(NC_2)_6$ framework are as follows:

A_g $$S_1 = \frac{1}{2\sqrt{3}} \sum_{i=1}^{12} \Delta s_i$$

$$S_2 = \frac{1}{\sqrt{6}} \sum_{i=1}^{6} \Delta r_i$$

$$S_3 = \frac{1}{\sqrt{6}} \sum_{i=1}^{6} \Delta \alpha_i$$

E_g $$S_{4a} = \frac{1}{2\sqrt{6}} (2\Delta s_1 + 2\Delta s_2 - \Delta s_3 - \Delta s_4 + 2\Delta s_5 + 2\Delta s_6 - \Delta s_7 - \Delta s_8 - \Delta s_9 - \Delta s_{10} - \Delta s_{11} - \Delta s_{12})$$

$$S_{5a} = \frac{1}{2\sqrt{3}} (2\Delta r_1 - \Delta r_2 + 2\Delta r_3 - \Delta r_4 - \Delta r_5 - \Delta r_6)$$

$$S_{6a} = \frac{1}{2\sqrt{3}} (2\Delta \alpha_1 - \Delta \alpha_2 + 2\Delta \alpha_3 - \Delta \alpha_4 - \Delta \alpha_5 - \Delta \alpha_6)$$

T_g $$S_{7a} = \frac{1}{2} (\Delta s_1 - \Delta s_2 + \Delta s_5 - \Delta s_6)$$

$$S_{8a} = \frac{1}{2} (\Delta \theta_{12} - \Delta \theta_{23} - \Delta \theta_{14} + \Delta \theta_{34})$$

$$S_{9a} = \frac{1}{\sqrt{2}} (\Delta \beta_1 - \Delta \beta_3)$$

$$S_{10a} = \frac{1}{\sqrt{2}} (\Delta \gamma_1 + \Delta \gamma_3)$$

$$S_{11a} = \frac{1}{\sqrt{2}}(\Delta\tau_1 + \Delta\tau_3)$$

A_u

$$S_{12} = \frac{1}{\sqrt{6}}\sum_{i=1}^{6}\Delta\beta_i$$

E_u $S_{13a} = \frac{1}{2\sqrt{3}}(2\Delta\beta_1 - \Delta\beta_2 + 2\Delta\beta_3 - \Delta\beta_4 - \Delta\beta_5 - \Delta\beta_6)$

T_u $S_{14a} = \frac{1}{\sqrt{2}}(\Delta s_1 - \Delta s_5)$

$$S_{15a} = \frac{1}{\sqrt{2}}(\Delta r_1 - \Delta r_3)$$

$$S_{16a} = \frac{1}{\sqrt{2}}(\Delta\theta_{12} - \Delta\theta_{34})$$

$$S_{17a} = \frac{1}{2}(\Delta\theta_{15} + \Delta\theta_{35} + \Delta\theta_{26} + \Delta\theta_{46})$$

$$S_{18a} = \frac{1}{\sqrt{2}}(\Delta\alpha_1 - \Delta\alpha_3)$$

$$S_{19a} = \frac{1}{\sqrt{2}}(\Delta\beta_1 + \Delta\beta_3)$$

$$S_{20a} = \frac{1}{\sqrt{2}}(\Delta\gamma_1 - \Delta\gamma_3)$$

$$S_{21a} = \frac{1}{\sqrt{2}}(\Delta\tau_1 - \Delta\tau_3)$$

The internal coordinates are defined as follows:

Δr_i = Δr(W–N)

Δs_i = Δr(N–C)

$\Delta\theta_{ij}$ = $\Delta\theta$(N$\hat{W}$N)

$\Delta\alpha_i$ = $\Delta\theta$(N$\hat{C}$N)

$\Delta\beta_i$ = N$\hat{C}$N wag

$\Delta\gamma_i$ = N$\hat{C}$N rock

$\Delta\tau_i$ = (NC_2) torsion

In the calculation only force constants associated with W–N stretching, N–C stretching and N$\hat{C}$N deformation were retained. Many of the interaction constants were equated to zero due to the paucity of wavenumber data. As a consequence of these approximations, only the diagonal F and G matrix elements are nonzero. Those used in the calculation are as follows:

A_g

$$F_{11} = f_s + f_{s*} + 8f_{ss} + 2f_{ss'}$$

$$F_{22} = f_r + 4f_{rr} + f_{rr'}$$

$$F_{33} = f_\alpha + 4f_{\alpha\alpha} + f_{\alpha\alpha'}$$

$$G_{11} = \mu_N(1 + \cos\alpha) + \mu_C$$

$$G_{22} = \mu_N$$

$$G_{33} = \frac{2}{s^2}(1 - \cos\alpha)\mu_N + \frac{2\mu_C}{s^2}$$

E_g

$$F_{44} = f_s + f_{s*} - 4f_{ss} + 2f_{ss'}$$

$$F_{55} = f_r - 2f_{rr} + f_{rr'}$$

$$F_{66} = f_\alpha - 2f_{\alpha\alpha} + f_{\alpha\alpha'}$$

$$G_{44} = G_{11}$$

$$G_{55} = G_{22}$$

$$G_{66} = G_{33}$$

T_u

$$F_{14,14} = f_s - f_{ss'}$$

$$F_{15,15} = f_r - f_{rr'}$$

$$F_{18,18} = f_\alpha - f_{\alpha\alpha'}$$

$$G_{14,14} = \mu_N + \mu_C$$

$$G_{15,15} = 2\mu_W + \mu_N$$

$$G_{18,18} = \frac{2}{s^2}(1 - \cos\alpha)\mu_N + \frac{2\mu_C}{s^2}$$

μ_C, μ_N and μ_W are the reciprocal masses of the carbon, nitrogen and tungsten atoms, r is the W–N bond length, s is the N–C bond length and α is the C$\hat{N}$C bond angle. Their values, obtained from ref. 3, are r = 2.032 Å, s = 1.515 Å ad α = 103°. The force constants are defined in Table III.